CMLS, Cell. Mol. Life Sci. 55 (1999) 639–652
1420-682X/99/040639-14 $ 1.50 + 0.20/0

CMLS Cellular and Molecular Life Sciences

Review

Structural properties of matrix metalloproteinases

W. Bode[a,*], C. Fernandez-Catalan[a], H. Tschesche[b], F. Grams, H. Nagase[c] and K. Maskos[a]**

[a]Max-Planck-Institut für Biochemie, D-82152 Martinsried (Germany), Fax + 49 89 8578 3516, e-mail: bode@biochem.mpg.de
[b]Universität Bielefeld, Abteilung Biochemie I, D-33615 Bielefeld (Germany)
[c]Department of Biochemistry and Molecular Biology, University of Kansas Medical Center, Kansas City (Kansas 66160, USA)

Received 18 November 1998; accepted 11 December 1998

Abstract. Matrix metalloproteinases (MMPs) are involved in extracellular matrix degradation. Their proteolytic activity must be precisely regulated by their endogenous protein inhibitors, the tissue inhibitors of metalloproteinases (TIMPs). Disruption of this balance results in serious diseases such as arthritis, tumour growth and metastasis. Knowledge of the tertiary structures of the proteins involved is crucial for understanding their functional properties and interference with associated dysfunctions. Within the last few years, several three-dimensional MMP and MMP-TIMP structures became available, showing the domain organization, polypeptide fold and main specificity determinants. Complexes of the catalytic MMP domains with various synthetic inhibitors enabled the structure-based design and improvement of high-affinity ligands, which might be elaborated into drugs. A multitude of reviews surveying work done on all aspects of MMPs have appeared in recent years, but none of them has focused on the three-dimensional structures. This review was written to close the gap.

Key words. Matrix metalloproteinases (MMPs); tissue inhibitors of metalloproteinases (TIMPs); crystal structures; proteinases; drug design.

The matrix metalloproteinases (MMPs, matrixins) form a family of structurally and functionally related zinc endopeptidases. Collectively, these MMPs are capable in vitro and in vivo of degrading all kinds of extracellular matrix protein components such as interstitial and basement membrane collagens, proteoglycans, fibronectin and laminin; they are thus implicated in connective tissue remodeling processes associated with embryonic development, pregnancy, growth and wound healing [1]. Normally, the degenerative potential of the MMPs is held in check by the endogenous specific (the tissue inhibitors of metalloproteinases, TIMPs) and nonspecific protein inhibitors (in particular α_2-macroglobulin). Disruption of this MMP-TIMP balance can result in pathologies such as rheumatoid and osteoarthritis, atherosclerosis, tumour growth, metastasis and fibrosis (for recent overviews, see e.g. [2–6]). Therapeutic inhibition of MMPs is a promising approach for treatment of some of these diseases, and the MMP structures and their TIMP complexes are therefore attractive targets for rational inhibitor design (for recent literature, see [7, 8]).

To date, 17 different human MMPs have been identified and/or cloned which share significant sequence homology and a common multidomain organization; several

* Corresponding author.
** Present address: Roche-Boehringer, D-68305 Mannheim (Germany).

counterparts have been found in other vertebrates, invertebrates and from plant sources (see [9]), together forming the MMP or matrixin subfamily A of the metalloproteinase M10 family [10]. According to their structural and functional properties, the MMP family can be subdivided into five groups: (i) the collagenases (MMPs-1, 8 and 13), (ii) the gelatinases A and B (MMPs-2 and 9), (iii) the stromelysins 1 and 2 (MMPs-3 and 10), (iv) a more heterogeneous subgroup containing matrilysin (MMP-7), enamelysin (MMP-20), the macrophage metalloelastase (MMP-12) and MMP-19 (together making up the 'classical' MMPs), and (v) the membrane-type MMPs (MT-MMPs-1 to -4 and stromelysin-3, MMP-11). These MMPs share a common multidomain structure, but are glycosylated to different extents and at different sites. According to sequence alignments [9, 11], the assembly of these domains might have been an early evolutionary event, followed by diversification [12].

All MMPs are synthesized with an $\sim$20-amino acid residue signal peptide and are (except probably the MT-MMP-like furin-processed proteinases [13–15]) secreted as latent pro-forms; these pro-proteinases consist of an $\sim$80-residue N-terminal pro-domain followed by the $\sim$170-residue catalytic domain (see figs 1 and 2), which in turn (except for matrilysin) is covalently connected through a 10- to 70-residue pro-rich linker to an $\sim$195-residue C-terminal haemopexin-like domain; in the MT-MMPs, the polypeptide chain possesses an additional 75- to 100-residue extension, which presumably forms a transmembrane helix and a small cytoplasmatic domain [14]. Removal of this haemopexin-like domain in the collagenases eliminates their characteristic capability to cleave triple-helical collagen, but does not significantly affect hydrolytic activity toward gelatin, casein or synthetic substrates (see [16]). In both gelatinases, the catalytic domains have an additional 175-amino acid residue insert comprising three fibronectin-related type II modules conferring gelatin and collagen binding.

The TIMP family currently includes four different members (TIMPs-1 to -4), which after optimal topological superposition exhibit 41–52% sequence identity (for references, see [22, 23]). Besides their inhibitory role, these TIMPs seem to have other functions such as growth factor-like and antiangiogenic activity (see e.g. [24, 25]). The TIMP complementary DNAs (cDNAs) encode an $\sim$25-residue leader peptide, followed by the 184- to 194-amino acid residue mature inhibitor. Virtually all TIMPs form tight 1:1 complexes with MMPs. Except for the rather weak interaction between TIMP-1 and MT1- and 2-MMPs [14, 26–28], the TIMPs do not seem to differentiate much between the various MMPs (see [29]). TIMPs-1 and -2 are unique in that they also bind to the pro-forms of gelatinase B and A, respectively [30]; the complex between MT1-MMP and TIMP-2 seems to act as a cell-surface-bound 'receptor' for progelatinase A activation in vivo, using these non-inhibitory interactions between TIMP-2 and progelatinase A [27, 31, 32]. Removal of the C-terminal one-third of the TIMP polypeptide chain gives rise to so-called N-terminal TIMP domains (N-TIMPs), which retain most of their reactivity toward their target MMPs [33, 34].

Only in early 1994 did the first X-ray crystal structures of the catalytic domains (blocked by various synthetic inhibitors) of human fibroblast collagenase/MMP-1 [35–37] and human neutrophil collagenase/MMP-8 [38, 39], and a nuclear magnetic resonance (NMR) structure of the catalytic domain of stromelysin-1/MMP-3 [40] become available, which were later complemented by additional catalytic domain structures of MMP-1 [41, 42], matrilysin/MMP-7 [43], MMP-3 [44–48], MMP-8 [49, 50] and MT1-MMP [22]. In 1995, the first X-ray structure of an MMP pro-form, the C-terminally truncated pro-stromelysin-1, was published [44, 47], and the

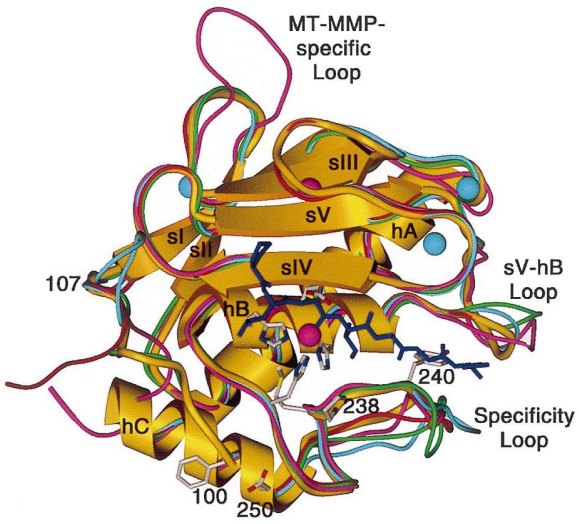

Figure 1. Ribbon structure of the MMP catalytic domain shown in standard orientation. The catalytic domain of the Phe100 form of MMP-8 [39] shown together with the modeled heptapeptide substrate (dark blue [49]) is superimposed with the catalytic domains of MMP-3 (blue [48]), MMP-1 (red [35]), MMP-14 (pink [22]) and MMP-7 (green [43]). The catalytic and the structural zinc (center and top) and the three calcium ions (flanking) are displayed as pink and blue spheres, respectively, and the three His residues liganding the catalytic zinc, the catalytic Glu in between, the characteristic Met, the Pro and the Tyr of the S1′ wall-forming segment, the N-terminal Phe and the first Asp of the Asp pair forming the surface-located salt bridge are shown with all nonhydrogen atoms. The chain segment forming the extra domain of both gelatinases will be inserted in the sV-hB loop (center, right) and presumably extends to the right side. Figure made with Setor [88].

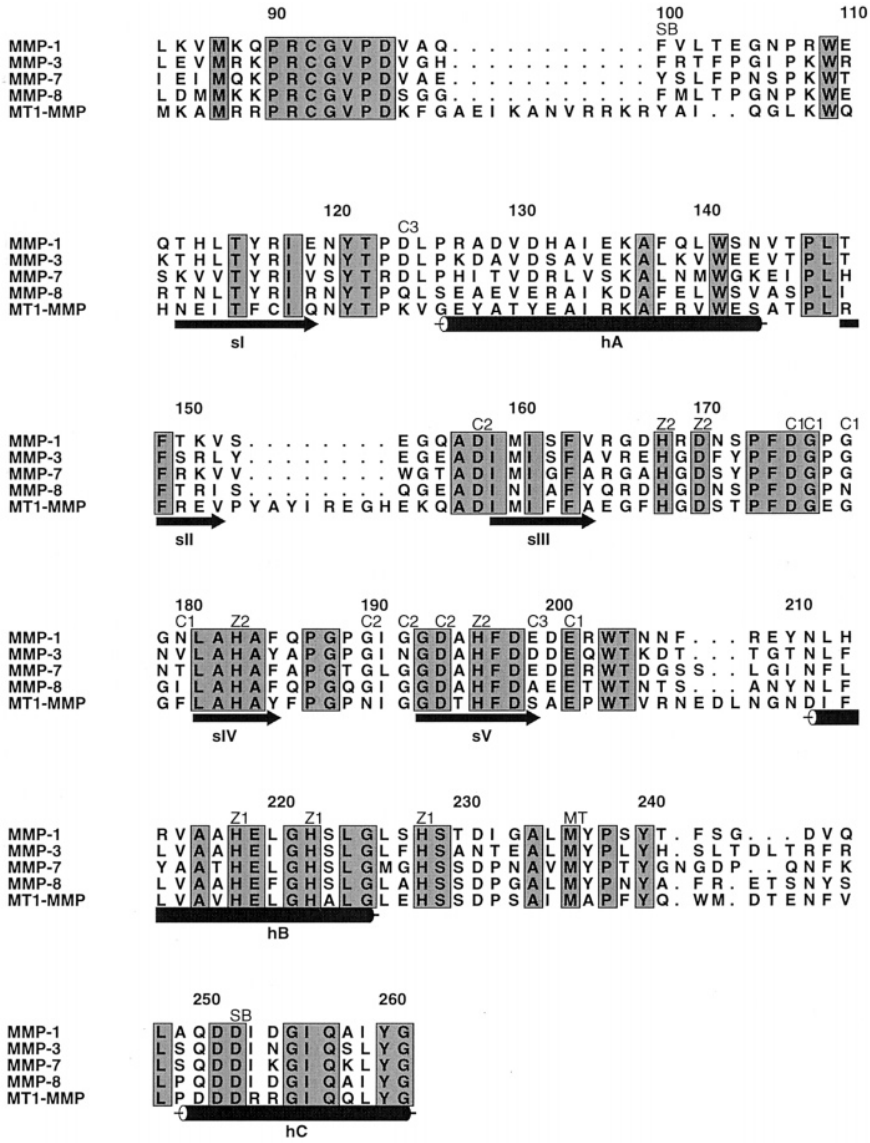

Figure 2. Sequence alignment of the catalytic domains of MMP-1 [17], MMP-3 [18], MMP-7 [19], MMP-8 [20] and MMP-14 [21], made according to topological equivalencies [22]. The numbering is that of the biosynthetic MMP-1 [17]. Location and extent of α-helices and β-strands are given by cylinders and arrows, and symbols show residues involved in main and side chain interactions with the catalytic (Z1) and the structural zinc (Z2), the first (C1), second (C2) and third calcium ion (C3) of the catalytic domains. Figure made with ALSCRIPT [89].

first and only structure of a mature full-length MMP, namely of porcine fibroblast collagenase/MMP-1 [51], was described. At that time, structures of the isolated haemopexin-like domains from human gelatinase A [52, 53] and from collagenase-3/MMP-13 [54] were also reported [55]. Of the TIMPs, a first preliminary NMR model of human N-TIMP-2 was presented in 1994 [56], which showed that the polypeptide framework of the N-terminal part of the TIMPs resembles so-called OB-fold proteins; a refined N-TIMP-2 has recently been published, describing some enhanced mobility of contacting inhibitor segments [57, 58]. In 1997, the first structure of a complete TIMP, human deglycosylated TIMP-1, in complex with the catalytic domain of human MMP-3, was published [48], followed by the X-ray structure of TIMP-2 in complex with the catalytic domain of MT1-MMP [22].

In the following sections, the structures of the MMPs and TIMPs and their detailed interactions will be presented. On the basis of topological equivalencies, structure-based sequence alignments will be given for the MMPs [22]. The MMP nomenclature used is based on the cDNA sequence of (human) fibroblast collagenase/MMP-1 [17] as the reference MMP (fig. 2). For the assignment of peptide substrate residues and substrate recognition sites on the proteinase, the nomenclature of Schechter and Berger [59] will be used: for example, P1, P2 and P1′, P2′ indicate the residues in N- and C-terminal direction of the scissile peptide bond of a bound peptide substrate (analogue), and S1, S2 and S1′, S2′ the opposite binding sites on the enzyme. TIMP residues will be given with TIMP-1/TIMP-2 numbers.

The MMP catalytic domain

The catalytic domains of the MMPs exhibit the shape of an oblate ellipsoid. In the 'standard' orientation, which in this article as well as in most other MMP papers is preferred for the display of MMPs, a small active-site cleft notched into the flat ellipsoid surface extends horizontally across the domain to bind peptide substrates from left to right (see fig. 4). This cleft harbouring the 'catalytic zinc' separates the smaller 'lower subdomain' from the larger 'upper subdomain'. This upper subdomain formed by the first three quarters of the polypeptide chain (up to Gly225) consists of a five-stranded β-pleated sheet, flanked by three surface loops on its convex side and by two long regular α-helices on its concave side embracing a large hydrophobic core (fig. 1). The polypeptide chain starts on the molecular surface of the lower subdomain, passes β-strand sI, the amphipathic α-helix hA, and β-strands sII, sIII, sIV and sV, before entering the 'active-site helix' hB (for nomenclature, see fig. 1). In the classical MMPs, strands sII and sIII are connected by a relatively short loop bridging sI; in the MT-MMPs, however, this loop is expanded into the spurlike, solvent exposed 'MT-MMP-specific loop' of hitherto unknown function. In all MMPs, strands sIII and sIV are linked via an 'S-shaped double loop', which is clamped via the 'structural zinc' and the first of two to three bound calcium ions to the β-sheet. This S-loop extends into the cleft-sided 'bulge' continuing in the antiparallel 'edge strand' sIV; this bulge-edge segment is of prime importance for binding of peptidic substrates and inhibitors (see fig. 3b). The sIV-sV connecting loop together with the sII-sIII bridge sandwiches the second bound calcium. After strand sV, the chain passes the large open sV-hB loop before entering the active-site helix hB; this helix provides the first (218) and the second His (222) which ligand the catalytic zinc, and the 'catalytic Glu219' in between, all of them representing the N-terminal part of the 'zinc-binding consensus sequence' HEXXH-XXGXXH (see fig. 2) characteristic of the metzincin superfamily [60, 61].

This active-site helix stops abruptly at Gly225, where the peptide chain bends down, descends (presenting the third zinc-liganding histidine, His228, and the following MMP-invariant Ser229, the function of which is not evident judged from the catalytic domain structure alone) and runs through a wide right-handed spiral (catalytic domain's 'chin') terminating in the 1,4-tight 'Met-turn' (of the strongly conserved sequence Ala234-Leu-Met236-Tyr237, with an obligatory methionine residue at turn position 3). The chain then turns back to the molecular surface to an (except in human stromelysin-3) invariant Pro238, forms with a conserved Pro238-X-Tyr240 segment (the 'S1′ wall-forming segment') the outer wall of the S1′ pocket, runs through another wide loop of slightly variable length and conformation (which due to fencing round the most important S1′ pocket and codetermining its extension might also be called the 'specificity loop', M. Browner personal communication), before it passes the C-terminal α-helix hC, which ends with the conserved Tyr260-Gly261 residue pair.

The overall structures of all MMP catalytic domains known so far are very similar, with the collagenase structures resembling one another most, and MMP-7 and the MT1-MMP structures deviating most (fig. 1). Larger main chain differences occur: (i) in the N-terminal segment up to Pro107 (depending on the length of the N-terminus and the presence of a TIMP); (ii) in the sII-sIII bridge (with the elongated and more exposed MT loop in the MT-MMPs); (iii) in the sV-hB loop; and (iv) in the specificity loop. With two (compared with MMP-7) and three (MMPs-1, -3 and -8) additional residues, the open sV-hB loop of MT1-MMP deviates most, followed by MMP-7; in both gelatinases, the approximately seven residues between Trp203–Thr204 and Leu/Phe/Ile212 are replaced by a 183-residue insert, which probably forms a large adjacent domain consisting of three tandem copies of fibronectin type II-like modules [62]; furthermore remarkable is the unusual cis conformation of the peptide bond preceding Tyr210 in MMPs-1 and -8, caused by the possibility of forming a favourable hydrogen bond with an adjacent strand [42, 49]. The specificity loop is shortest in MMP-1; those of MMPs-3, -8 and -14 (with three and two additional residues) resemble one another, whereas that of MMP-7 (two) deviates most (figs 1 and 2).

Besides the catalytic zinc, all MMP catalytic domains possess another zinc ion, the structural zinc, and two (MMP-8, MT1-MMP) or three bound calcium ions (MMP-1, MMP-3, MMP-7) (figs 1 and 2). The structural zinc and the first (probably most tightly bound)

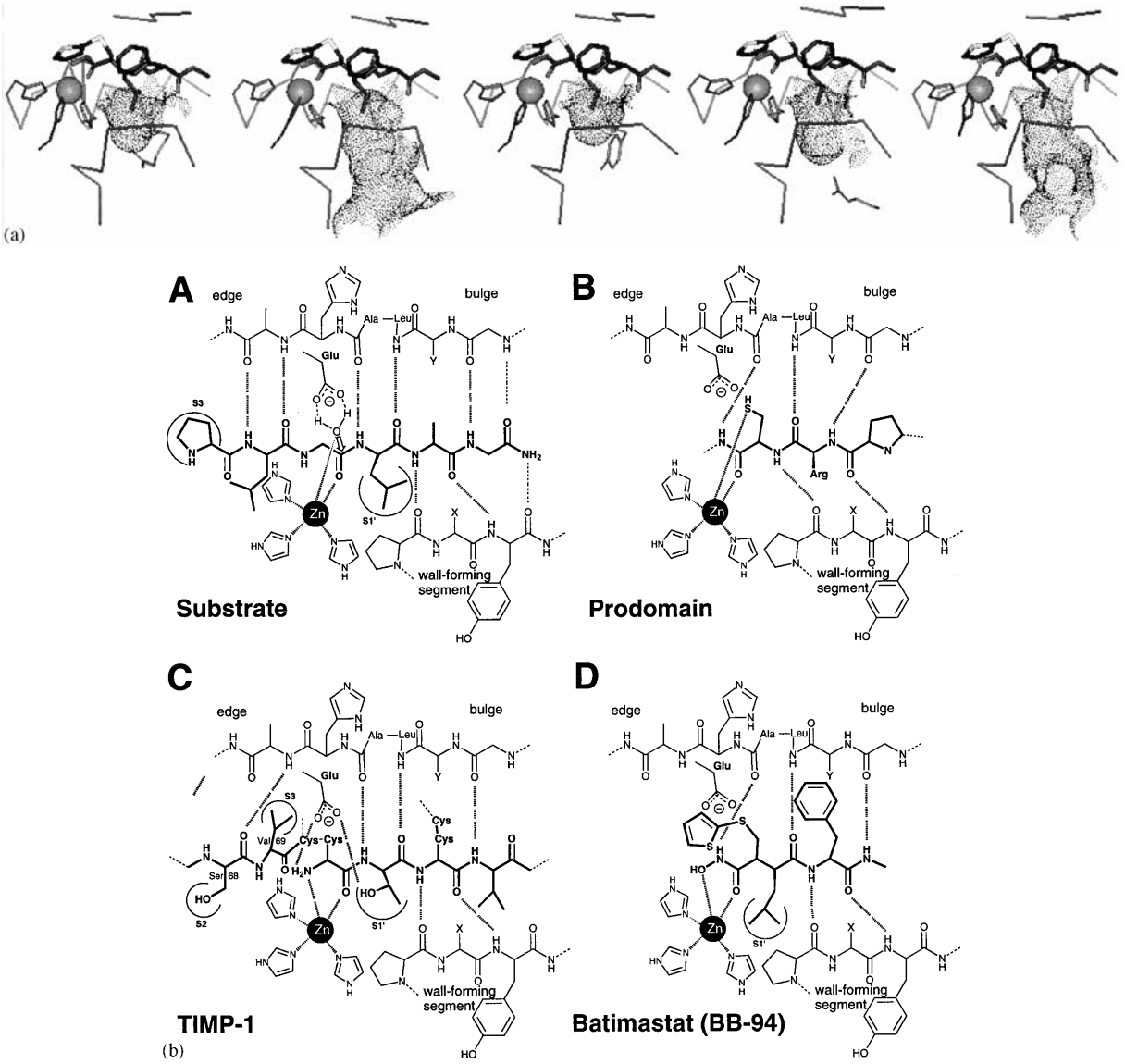

Figure 3. Peptide substrate and inhibitor interaction and specificity. (*a*) Comparison of the S1′ pockets (dot surface) of (from left to right) MMP-1, MMP-3, MMP-7, MMP-8 and MMP14. Besides the Cα plots of the bulge-edge strand (dark-grey, top), of the active-site helix (light grey, center) and the segment comprising the Met-turn and the S1′ wall-forming segment (dark grey, bottom), the full structure of the inhibitor lead batimastat [4-(N-hydroxyamino)-2(R)-isobutyl-3(S)-[(2-thienyl-thiomethyl)succinyl]-L-phenylalanine-N-methylamide] alias BB-94 (as bound to MMP-8 [49]), the catalytic zinc (sphere), the side chains of the three zinc-liganding His residues, and the side chains of residues Arg214, Tyr214 and Arg243 restricting the S1′ pockets of MMP-1, MMP-7 and MMP-8, respectively, in size are shown. (*b*) Schematic drawing of the putative encounter complex between (A) a modeled Pro-Leu-Gly-Leu-Ala-Gly-amide hexapeptide substrate [48], (B) the pro-domain switch peptide [43], (C) the N-terminal segment and the C-connector loop of TIMP-1 [47] and (D) batimastat [49] and the MMP active site. The substrate polypeptide chain, the switch peptide, the N-terminal segment and the inhibitor peptide mimic (bold connections) run antiparallel to the bulge-edge strand (top) and parallel to the S1′ wall-forming segment (bottom), forming several inter-main-chain hydrogen bonds (dashed lines). Dominant hydrophobic interactions are made through the substrate's P1 and P3 side chains with the S1′ pocket and the S3 subsite (emphasized through two troughs). In the enzyme-substrate encounter, the catalytic water activated by the catalytic Glu residue is suitably placed and activated to attack the carbonyl group of the scissile P1-P1′ peptide bond. Figure made with InsightII.

calcium are sandwiched between the double-S loop and the outer face of the β-sheet. In the vast majority of the classical and the furin-activatable MMPs, the structural zinc is coordinated by the imidazoyl Nε2 or Nδ1 atoms,

respectively, of three His residues (provided by the S-loop, sIV and sV) and by one carboxylate oxygen of the Asp residue in the S-loop next but one to the liganding His residue (see fig. 2). This zinc is completely buried in the protein matrix; the impossibility of exchanging it in the MMP-8 crystals [38] suggested its extremely tight binding. The second part of the S-loop encircles the adjacent calcium ion and packs it against the side chain carboxylate groups of an invariant Asp-Glu couple protruding from strand sV; these carboxyl oxygens, together with three carbonyl and one carboxyl oxygen of the S-loop, coordinate this calcium in a nearly octahedral manner. The second calcium ion, sandwiched between the sIV-sV loop and sIII, is octahedrally coordinated by three carbonyl groups, a bulk solvent and one carboxylate oxygen of the invariant Asp at the start of strand sV. The loop immediately following sV encircles the third calcium and coordinates it through two carbonyl groups (of residues 199 and 201, fig. 2) and one carboxylate oxygen of Asp124, whose presence seems to correlate with the existence of a third calcium site.

For the fibroblast and the neutrophil collagenases, a severalfold larger activity has been demonstrated for active enzymes, starting with a highly conserved Phe100 residue compared with species truncated for one or two residues (a phenomenon also called 'superactivity' or 'superactivation' [63, 64], reviewed in [65]). Position and fixation of the N-terminus of the mature classical MMPs seem indeed to depend on the presence of the N-terminal amino acid Phe/Tyr100, that is on the accurate processing/tailoring of the MMP precursor [38, 39]. In cases where it starts with (the highly conserved) Phe100 (see fig. 2), the N-terminal heptameric segment preceding the conserved Pro107-Lys/Arg-Trp109 triple is tightly packed against a hydrophobic surface groove made by the C-terminal helix hC and the descending segment centering around the third His ligand of the catalytic zinc; the N-terminal Phe100 ammonium group makes a surface-located salt bridge with the side chain carboxylate of an Asp250, which is the first residue of a strictly invariant helix hC-based Asp250-Asp251 pair [39]. The side chain of the second of both Asp residues is buried in a solvent-filled protein cavity and hydrogen-bonded via the Met-turn to the first zinc-liganding His. Along this path, formation of the Phe100...Asp250 salt bridge might be signaled to the active center. In the absence of an N-terminal Phe/Tyr100 (a state associated with a lower catalytic activity), the N-terminal (hexa)peptide preceding Pro107 is disordered and might interfere with substrate binding, offering an alternative explanation for the reduced activity of such N-terminally truncated MMPs.

Specificity determinants

Bounded at the upper rim by the bulge-edge segment and the second part of the S-loop, and at the lower side by the third zinc-liganding imidazole and the S1′ wall-forming segment, the active-site cleft of all MMPs is relatively flat at the left ('nonprimed') side, but carves into the molecular surface at the catalytic zinc and to the right ('primed') side, leveling off again to the surface further to the right (see fig. 4). In its center and to the right side, this cleft exhibits a slightly negative potential. In unliganded MMPs, the catalytic zinc residing in its center is coordinated by the three imidazole Nε2 atoms of the three histidines (His218, 222 and 228) and by a fixed water molecule, which simultaneously is in hydrogen bond distance to the carboxylate group of the catalytic Glu219. In case of MMP complexes with bidentate inhibitors (such as those with a hydroxamic acid function, see figs 3a,b), this water is replaced by two oxygen atoms, which together with the three imidazoles ligand the catalytic zinc in a trigonal-bipyrimidal (pentacoordinate) manner [38]. As in all other metzincins [60, 61], the zinc-imidazole ensemble of the MMPs is placed above the distal ε-methyl-sulfur moiety of the strictly conserved Met236 of the Met-turn, which forms a hydrophobic base of still unclear function (see fig. 1). An MMP-8 catalytic domain with this Met replaced by a selenomethionine retained its catalytic activity, and exhibited slightly decreased kinetic and thermal properties but (except for a slight local disturbance) virtually no conformational differences compared with the wild-type domain [66].

Immediately to the right of the catalytic zinc, the S1′ specificity pocket invaginates, which in size and shape considerably differs among the various MMPs (fig. 3a). This pocket is mainly formed (seen in standard orientation) by (i) the initial part of the active-site helix hB ('back side'), (ii) the somewhat mobile [45] phenolic side chain of Tyr240 ('right-hand flank'), (iii) the main chain atoms of the underlying wall-forming segment Pro-X-Tyr ('front side'), (iv) the flat side of the first zinc-liganding His218 imidazole ('left side') and (v) the Leu(Ile/Val)235 residue of the Met-turn, which together with the Leu/Tyr/Arg214 or the Arg243 side chain (if present) form its 'bottom' or line it towards the second exit opening at the lower molecular surface, respectively. In all MMPs, the interior of the pocket has direct water-mediated connections to the bulk water; this pocket is, however, of quite different size and shape depending on the presence of a Leu, a Tyr or an Arg at position 214 (see below).

Nearly all of the synthetic inhibitors analyzed so far in MMP complexes contain a chelating group (such as a hydroxamic acid, a carboxylate or a thiol group) for zinc ion ligation, and a peptidic or peptidomimetic

moiety mimicking peptide substrate binding to the substrate recognition site. Of the synthetic inhibitors published in complex with an MMP, only the Pro-Leu-Gly-hydroxamic acid inhibitor [38, 39] binds to the left-hand subsites (the nonprimed subsites S3 to S1) alone, antiparallel to the edge strand ('left-side inhibitor'). A few synthetic inhibitors bind across the active site, whereas in the majority of synthetic inhibitors studied so far this peptidic moiety interacts in an extended manner with the primed right-hand subsites ('right-side inhibitors'), inserting between the (antiparallel) bulge-edge segment and the (parallel) S1′ wall-forming segment of the cognate MMP under formation of a three-stranded mixed β-sheet (see panel D in fig. 3b).

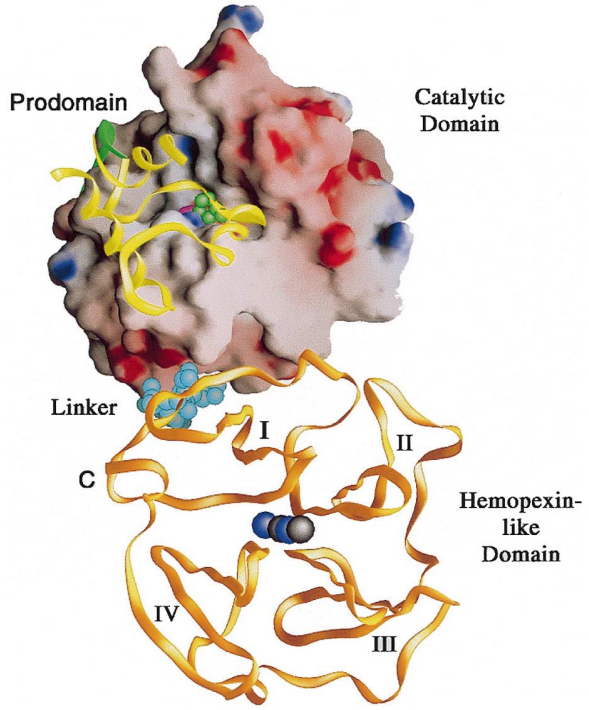

Figure 4. Modeled structure of the full-length proMMP. The catalytic domain is shown in standard orientation. The pro-domain and the catalytic domain are taken from the experimental proMMP-3 catalytic domain structure [44], whereas the linker (blue spheres) and the haemopexin-like domain are taken from and attached as seen in the crystal structure of full-length MMP-1 [51]. The catalytic domain from the hinge residue, Pro107, onwards is given as a solid surface colored according to the electrostatic surface potential. In the center of the active-site cleft running from left to right resides the catalytic zinc (pink half sphere, center). The pro-segment is shown as a yellow ribbon with its ordered segments only, that is with the first (only apparently separated) helix, the second helix, the connecting loop, the third helix and the switch loop (running across the catalytic zinc liganding it via the conserved Cys side chain, shown as a green CPK model), and the rocker arm (green color), which swings to the bottom left after activation cleavage. The haemopexin-like domain consisting of the four blades I to IV and viewed at its exit side is shown as a golden ribbon; the single calcium ion (blue sphere, back) located at the entry side (MMP-1) is shown together with the second calcium (central blue sphere) and the two chlorine ions (black spheres) found in the haemopexin-like domains of gelatinase A and MMP-13. Figure made with GRASP [77].

An L-configurated P1′-like side chain is perfectly arranged to extend into the hydrophobic bottleneck of the S1′ pocket. This P1′-S1′ interaction is the main determinant for the affinity of inhibitors and the cleavage position of peptide substrates. Depending in particular on the length and character of residue 214 harboured in the N-terminal part of the active-site helix hB, the size of the S1′ pocket differs considerably among the MMPs (fig. 3a). In MMP-1 and MMP-7, the side chains of Arg214 and Tyr214, respectively, extend into the S1′ opening, limiting it to a size and shape still compatible with the accommodation of medium-sized P1′ residues, but less for very large side chains, in agreement with peptide cleavage studies on model peptides [67–69]. Some more recent MMP-1 structures show, however, that the Arg214 side chain can swing out of its normal site, thus also allowing binding of synthetic inhibitors with larger P1′ side chains (M. Browner, personal communication). The smaller Leu214 residues of MMP-3 and MMP-14 (and probably also of MMPs-2 and -9) do not bar the internal S1′ 'pore', which extends right through the molecule to the lower surface, that is equals more a long solvent-filled 'tube' (fig. 3a). In spite of a small Leu214 residue, however, the S1′ pocket of MMP-8 is of medium size and is closed at the bottom, due to the Arg243 side chain extending into the S1′ space from the specificity loop [38].

Second in importance for substrate specificity seems to be the interaction of the P3 residue (in collagen cleavage sites always a Pro residue), with the mainly hydrophobic S3 pocket (fig. 3b). The S2 site is a shallow depression extending on top of the imidazole ring of the second zinc-liganding His; its polarity character might be influenced by residue 227 preceding the third zinc-liganding His, His228. Longer side chains of P1 residues (in collagen cleavage sites mostly a Gly, for references see [70]) are placed in the surface groove lined by the His183 side chain of the edge strand together with the last bulge residue 180 (marked with a 'Y' in fig. 3b); depending on this latter side chain, one or the other P1 side chain might be preferred. P2′ side chains extend away from the surface, squeezed between the bulge rim and the side chain of the middle residue of the Pro-X239-Tyr wall-forming segment; the quality of interaction will be determined particularly by the nature of bulge residue 180 and residue 239 (marked with an 'X' in fig. 3b), which in the MMPs-14, -15 and -16 and MMP-11 is an exposed Phe [22]. Further to the right side the molecular surface again has a hydrophobic/po-

lar depression, which could accommodate P3′ side chains of differing nature (see the accomodation of residue 4 of bound TIMPs in panel C of fig. 3b).

By replacing the zinc-chelating groups of such peptidic left- and right-side inhibitors by a normal peptide bond, a contiguous peptide substrate was constructed, indicating the probable binding geometry of a normal substrate-MMP encounter complex (panel A in fig. 3b) [49]. Accordingly, the peptide substrate chain is aligned in an extended manner to the continuous bulge-edge segment, under formation of an antiparallel two-stranded β-pleated sheet, which expands on the right-hand side into a three-stranded mixed parallel-antiparallel sheet due to additional alignment with the S1′ wall-forming segment. The bound peptide substrate (such as the hexapeptide shown in fig. 3b) forms five and two inter-main chain hydrogen bonds, respectively, to both crossing-over MMP segments. Similar to the reaction mechanism previously suggested for the more distantly related zinc endopeptidase thermolysin [71], the MMP catalyzed cleavage of the scissile peptide bond will probably proceed via a general base mechanism [49]. The carbonyl group of the scissile bond (Gly-Phe in fig. 3b) is directed nearly toward the catalytic zinc and strongly polarized. The zinc-bound water molecule is activated by the carboxylate/carboxylic acid of the catalytic Glu219, the pK of which might (in particular after complete shielding from the bulk water upon substrate/inhibitor binding) be shifted to higher values, due to packing in the protein matrix without charge-stabilizing internal hydrogen bonds (the importance of this Glu219 for proteolytic activity in MMPs has been demonstrated through replacement with Asp, Ala and Glu residues [72, 73], resulting in mutants with lowered or extremely low catalytic activity, respectively). This activated water molecule squeezed between the carboxylate group of the catalytic Glu and the scissile peptide bond carbonyl group is properly oriented to attack via its lone pair orbital the electrophilic carbonyl carbon. The tetrahedral intermediate is presumably stabilized by both the zinc and the carbonyl group of the first Ala residue of the edge strand sIV. Simultaneously, one water proton could be transferred via the Glu carboxylate (acting as a proton shuttle) to the amino group, which after break of the peptide bond and transfer of a second proton could leave the enzyme-substrate complex together with the N-terminal substrate fragment. Remarkably, there is no other electrophil (such as His231 in thermolysin [71] or Tyr149 in astacin [74, 75]) in the catalytic zinc environment of the MMPs, which could further stabilize the carboxy anion of the presumed tetrahedral intermediate; a frequently observed water molecule suggested to be activated by the carbonyl group of Pro238 [43] does not seem to be able to take over this role.

The MMP Pro-domain

Currently, the only pro-MMP structure known to date is that of the C-terminally truncated MMP-3 [44, 47]. The pro-peptide has an egglike shape, attached with its rounded-off side to the active site of the catalytic domain. It essentially consists of three mutually perpendicularly packed α-helices and a segment connecting it with the catalytic domain (see fig. 4). The $\sim$15-residue-long solvent-exposed N-terminal segment is flexible; the polypeptide chain is first defined in helix 1, which it connects through a mostly disordered surface-located segment with the four-turn α-helix 2 directed toward the 'chin' of the catalytic domain; the pro-chain then deviates from the catalytic domain surface through a defined multiple-turn loop, turns back through helix 3 to the conserved Pro90, where it kinks and enters the active-site cleft as the almost invariant Pro90-Arg-Cys-Gly-Val-Pro-Asp96 'switch segment'; this loop (with the first three residues and the Asp strictly conserved, and with only a very few variations in the residual three residues) is similarly arranged as, but with opposite direction to a bound P3′ to P2 peptidic substrate down to the Val residue, that is it aligns parallel to the bulge-edge segment and antiparallel to the S1′ wall-forming segment under formation of five inter-main chain hydrogen bonds (panel B in fig. 3b). At the conserved Val residue, the pro-peptide chain kinks away from the catalytic domain surface, turns back and runs via the final X99-Phe/Tyr100 cleavage site (which in this static structure is neither accessible nor in a suitable proteinase-binding conformation) into the 'rocker arm' (see fig. 4), which terminates at the strongly conserved Pro107. From this Pro residue onwards the polypeptide chain of the pro-MMP is in register with that of the mature, that is activated, MMPs. In MMP-11 and in the four MT-MMPs, up to 11 residues are inserted between the switch loop of the pro-chain and the catalytic domain, and the pro-chain terminates in an Arg-X-Arg/Lys-Arg sequence typical for cleavage by furin-like convertases [14, 76]; intracellular cleavage of the MT-MMPs and MMP-11 by Golgi-associated furin-like enzymes results in expression of the active enzymes [15].

The bent switch segment is bridged by the side chains of the strictly conserved residues Arg91 and Asp96, whose side chains are turned toward one another under formation of a symmetric 2N...2O salt bridge located on top of the third zinc-liganding His228; from the propeptide side, this salt bridge is sandwiched by the phenol side chains of (up to) three strongly conserved Tyr residues presented by helices 1 and 2, which shield it against the bulk water and strengthen the pro-domain-catalytic domain interaction as long as the pro-domain is intact. Somewhat similar to P2′ and P1′ side chains of bound

peptide substrates, the Arg and Cys side chains are directed away from the active-site cleft and toward the S1′ pocket, respectively, with the Sγ of the latter turned to the catalytic zinc, however, acting as the fourth ligand in a tetrahedral coordination sphere (fig. 3b). In spite of the bound pro-domain, the entire active-site region of the catalytic domain of this pro-form is remarkably similar in structure to that in the mature enzyme.

Pro-MMP activation by (other) proteinases (see [65]) seems to proceed via a stepwise mechanism: some early cleavages occurring in the flexible, exposed helix1-helix2 loop (the 'bait') not only might expose the hydrophobic core of the pro-chain domain, but in particular also destabilize this domain, thus exposing other (downstream) cleavage sites and weakening and finally destroying the Cys-catalytic zinc interaction, eventually leading to a liberation and flexibilization of the X99-Phe/Tyr100 activation cleavage peptide bond (as originally predicted by the 'cysteine switch hypothesis' [78]); this segment then might adapt and bind to the substrate binding site of an approaching cleaving proteinase. In the case of liberation of a Phe/Tyr100 N-terminus (in the classical MMPs), the activation cleavage seems to be accompanied by substantial rearrangement of the N-terminal 100–107 rocker arm (see fig. 4) into the surface crevice described above; the N-terminal residue moves for about 17 Å to form the above-mentioned surface-located salt bridge with the carboxylate of Asp250 of the helix C-based Asp250/Asp251 pair; in this movement, the Pro107 residue acts as a flexible joint, with its main chain angles changing from an α-helix-like (in the pro-form) to a polyproline-II-like conformation (in the mature form).

It might be worth noting that the MMP pro-peptides are not required for proper (re)folding of the catalytic domains, in contrast to some other pro-proteinases [47].

The haemopexin-like MMP domain

Except for MMP-7, all vertebrate and human MMPs are expressed with a C-terminal haemopexin-like domain. Some of these haemopexin-like domains have been shown to be involved in substrate recognition and to confer substrate specificity, most dramatically in the collagenase subfamily, where the capability to cleave native triple-helical collagen is associated with the covalently bound haemopexin-like domain (for references, see [16]). In the MT-MMPs, these haemopexin-like domains have a 75- to 100-residue extension, which seems to constitute a connecting peptide, a transmembrane segment and a short cytoplasmatic fragment [14].

The haemopexin-like domains of the classical MMPs exhibit the shape of an oblate ellipsoidal disc and exhibit very similar structures [51–54]. The haemopexin-like domain polypeptide chain (with an early recognized sequence similarity with haemopexin, a plasma haem binding and transporting protein, see [79]) is essentially organized in the four β-sheets (blades) I to IV, which are arranged almost symmetrically around a central axis in consecutive order, giving rise to the formation of a four-bladed propeller of pseudo-fourfold symmetry (fig. 4). Each propeller blade is made by four antiparallel β-strands connected in a W-like topology, and is strongly twisted. The first innermost strands in all four blades enter the propeller at one side (the 'entrance side') and run almost parallel to one another along the propeller axis, forming a central funnel-shaped tunnel, which opens slightly toward the exit. The fourth strands of blades II and III are interrupted by characteristic β-bulges, which allow these strands to keep in phase with the antiparallel third strands in spite of the overall sheet curvature. In all four blades, the outer segments loop around the periphery of the disc and end up in short helical segments. The C-terminus of the blade IV helix is tethered to the entering strand of blade I via the single disulfide bridge, stabilizing the whole domain. In spite of the strong volume increase in radial direction, the haemopexin-like domain ellipsoid is evenly filled with protein mass, mainly achieved by a general increase in the size of the amino acid residues when going from the center to the periphery.

Within the central tunnel, up to four heavier ions have been identified. At the entrance to this tunnel a calcium ion is placed (in the back of fig. 4), which is tetragonally surrounded by the first carbonyl group of each of the four inner strands. The center of the tunnel harbours an ion pair, which has been interpreted as a chloride-calcium couple. The calcium ion is octahedrally surrounded by the four carbonyl oxygens of the four residues positioned third in the innermost strands, and by the chlorine and a second chlorine/water molecule on both sides. The chlorine ion, situated between both calcium ions, is tetrahedrally coordinated by the nitrogen atoms of the same amide groups, which also ligand the second calcium [53]. The function of these ions is not yet clear. In the three different haemopexin-like domain structures known so far, the charge patterns differ more than the surface contours (see [54]). In this respect, the haemopexin-like domains from the collagenases show particularly strong similarities to one another. In all haemopexin-like domains (up to four) charge-uncompensated Asp residues are arranged around the tunnel entrance. On the exit side of the MMP-2 haemopexin-like domain, a surface patch of positively charged residues is noteworthy, which might be involved in binding to TIMP-2 [53]; however, some novel mutagenesis studies locate the TIMP-2 binding site to the junction of blades III and IV on the periph-

eral rim of the MMP-2 haemopexin-like domain (C. Overall, personal communication).

In the full-length MMP-1 structure [51], the catalytic domain and the hemopexin-like domain make noncovalent contacts only along small domain edges, with the outermost strand of the first blade of the haemopexin-like domain propeller contacting the C-terminal helix hC of the catalytic domain (fig. 4). The 17 (or 12 depending on counting) amino acid residue 'linker' between both domains bulges backwards and runs in a loose manner antiparallel to helix hC, before it joins (about four residues before the first Cys residue) the haemopexin-like domain moiety. This linker is rich in Pro residues, but is quite flexible and thus a preferred target for hydrolytic cleavage [51]. Chimeric constructs made to define the structural features encoding the triple-helicase specificity of collagenases [80–82] show that both the catalytic domain and the haemopexin-like domain have important determinants, and that both must be suitably linked to act in concert to confer helicase specificity. It has been suggested that after binding of the triple-helical substrate to the MMP-1 and -8 catalytic domains, the fully stretched linker (acting like a spacer) would just allow the haemopexin-like domain to fold over the catalytic domain, sandwiching, trapping and (possibly) destabilizing the substrate [54]. However, MT1-MMP, also exhibiting triple-helicase activity [83], exhibits a much longer linker (reviewed in [16]). Alanine scanning experiments with MMP-8 [84] indeed show that also the linker sequence motif, with special emphasis on the Pro residues, is important to retain the collagenolytic activity. Hopefully, structures of full-length MMPs in complex with heterotrimeric collagen-like peptides, which are preferentially cleaved by full-length collagenases [85], will help to solve this controversial issue in the future. Modeling experiments have shown that collagen-like triple-helical structures are far too bulky and that each constituent single strand is not in an appropriate conformation to allow a productive cleavage interaction with the MMP catalytic site, and that the scissile strand of triple-helical collagen must be freed for productive binding [38].

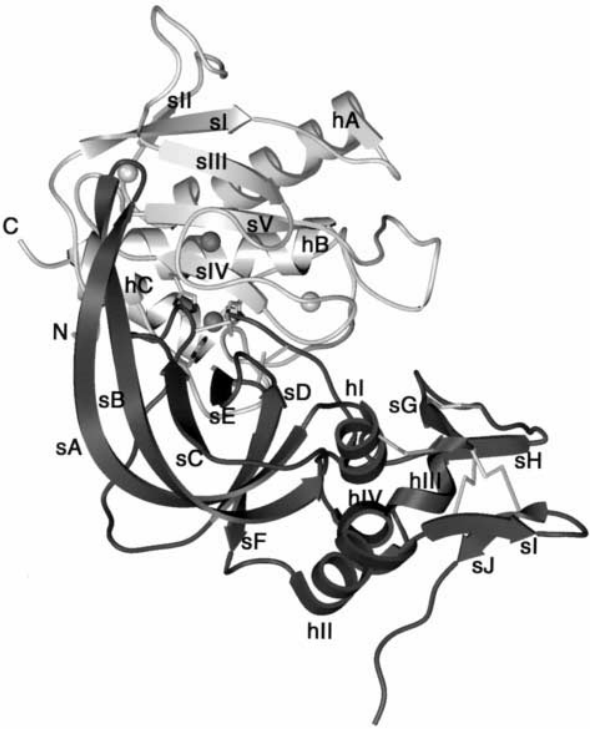

Figure 5. MMP-TIMP complex. The complex formed by the MT1-MMP catalytic domain (top) and TIMP-2 (bottom) [22] is displayed in front view. All disulfide bridges are given, and the zinc and calcium ions are represented as dark grey and light grey spheres. The wedge-shaped inhibitor binds with its edge made by six segments into the entire active-site cleft of the MMP-3, which in this view is directed toward the bottom. The N-terminal Cys1 of TIMP-1 is located on top of the catalytic zinc, and the first five N-terminal residues bind to the active site in a substrate-like manner. Figure made with Setor [88].

TIMP structure and TIMP-MMP interaction

The TIMPs have the shape of an elongated contiguous wedge consisting of an N-terminal segment (Cys1 to Pro5), an all-β-structure left-hand part, an all-helical center and a β-turn structure to the right (according to the front view in fig. 5) [48]. The N- and the C-terminal halves of the polypeptide chain form two opposing subdomains. The N-terminal subdomain exhibits a so-called OB-fold, known for a number of oligosaccharide/oligonucleotide binding proteins [56]. This region consists of a five-stranded β-pleated sheet of Greek-key topology rolled into a closed β-barrel of elliptical cross-section. The narrower opening of this barrel is bounded by the sB-sC loop, while its wider exit is, in contrast to other OB-fold proteins, covered by an extended segment connecting strands sC and sD, designated as 'connector' [48]. After leaving the barrel, the polypeptide chain passes two helices, forms a two-stranded β-sheet, runs through a wide multiple-turn loop and terminates in a β-hairpin sheet. The last 3 (TIMP-1) to 10 (TIMP-2) C-terminal residues do not exhibit a defined conformation and presumably form a flexible tail on the TIMP surface [22, 48].

The TIMP edge is formed by five sequentially separate chain segments, namely the extended N-terminal segment Cys1-Pro5 flanked by the sA-sB loop and the sC-connector loop on the left-hand side, and by the sG-sH loop and the multiple-turn loop on the right-

hand side (fig. 5). The N-terminal segment is tightly connected to the adjacent sC-connector and to the underlying sE-sF loop via disulfide bridges Cys1–Cys70/72 and Cys3–Cys99/101. Particularly remarkable features of TIMP-2 are the quite elongated sA-sB β-hairpin loop, which does not follow the OB-barrel curvature but is twisted and extends away, and the much longer negatively charged flexible C-terminal tail. TIMP-4 seems to share these features with TIMP-2, whereas TIMP-3 should exhibit a short sA-sB loop and a long but not negatively charged tail [22, 23]. Altogether, the TIMP topologies differ considerably, in spite of 40% overall sequence identities.

In complexes with MMPs, the wedged-shaped TIMPs bind with their edge into the entire length of the active-site cleft of their cognate MMPs [22, 48] (fig. 5), under removal of about 1300 Å^2 surfaces of each molecule from contact with bulk water and some rigidification of the participating loops [58] upon complex formation. The majority of all intermolecular contacts is made by the N-terminal segment Cys1-Pro5, the sC-connector loop and the connecting disulfide bridge; in case of TIMP-2, the participation of the sA-sB loop in intermolecular contacts is considerable. The first five TIMP residues Cys1 to Pro5 bind to the MMP active-site cleft in a substrate- or product-like manner, that is similar as P1, P1′, P2′, P3′ and P4′ peptide substrate residues insert between the bulge and the wall-forming segments, forming five intermolecular inter-main chain hydrogen bonds (see panel C in fig. 3b). The sC-connector loop, in particular residues Ser68/Ala70 and Val69/Leu71, in contrast, interacts in a somewhat substrate-inverse manner with the left-hand subsites S2 and S3 [22, 48].

Cys1 is located directly above the catalytic zinc, with its N-terminal α-amino nitrogen and its carbonyl oxygen atoms placed directly above the catalytic zinc, coordinating it together with the three imidazole rings from the cognate MMP. The α-amino group of Cys1 approximately occupies the site of the bound 'attacking' water molecule and forms a hydrogen bond to one carboxylate oxygen atom of the catalytic Glu219. In spite of this close interaction, the Glu219Asp mutation in MMP-2 does not significantly affect TIMP-1 binding [72]. The Thr/Ser side chain of the second TIMP residue extends into the S1′ pocket of the cognate MMP, similar to the side chain of a P1′ peptide substrate residue (fig. 3b), without filling this pocket properly; the Thr/Ser2 side chain oxygen is hydrogen-bonded to the catalytic Glu219 carboxylate of the target MT1-MMP; mutagenesis experiments with N-TIMP-1 have shown that replacement of Thr2 by other natural amino acids can lead to TIMP species, which are able to discriminate much more between different MMPs [33]. The Cys3, Val/Ser4 and Pro5 side chains touch subsites S2′, S3′ and S4′ in a manner expected for substrate P2′, P3′ and P4′ side chains (see fig. 3b). It is noteworthy that a very similar substrate-like interaction has been found in two crystal forms of 'noninhibited' MMP-1 catalytic domains [40], where the opened-out N-terminal segment (Leu102-Thr-Glu-Gly105) of one molecule inserts into the S1 to S3′ subsites of a symmetry-related molecule, utilizing identical subsite and intermolecular hydrogen bond interactions as observed in the MMP-TIMP complexes.

In the MT1-MMP-TIMP-2 complex (fig. 5), the quite long sA-sB hairpin loop of TIMP-2 folds alongside the S-loop over the rim of the active-site cleft and reaches up to the β-sheet of its cognate MMP [22]; in spite of the relatively large overall interface between the sA-sB loop and the molecular MMP surface, most of the intermolecular contacts do not seem to be designed for optimal complementarity, however. The other edge loops of TIMP are involved in a relatively small number of intermolecular contacts, with both C-terminal edge loops (in particular in TIMP-1) showing relatively high flexibility. Binding data indicate, however, that the interaction of the C-terminal TIMP subdomains with a cognate MMP might be of much greater importance for the TIMP inhibition of the gelatinases and MMP-13 [16], probably correlating with tighter intermolecular contacts.

Superposition experiments with the structure of full-length porcine MMP-1 [51] show that the C-terminal haemopexin-like domain of full-length MMPs as positioned in that structure would be compatible with TIMP binding [48]. In such a TIMP-full-length MMP complex both domains, the TIMP and the haemopexin-like domain would just touch one another, in agreement with kinetic binding studies showing [except for gelatinases A and B and MMP-13 (see [16])] that the C-terminal MMP domains contribute relatively little to TIMP binding [29, 33]. The negatively charged C-terminal tail of TIMP-2 seems to facilitate noninhibitory binding to the progelatinase A haemopexin-like domain mainly via electrostatic interactions. This specific TIMP-2 tail-MMP-2 haemopexin-like domain interaction is important for formation of the MT1-MMP-TIMP-2-progelatinase complex implicated in progelatinase activation [86, 87].

Acknowledgements. We thank Drs E. Madison and R. Huber for valuable discussions. Financial support from the Sonderforschungsbereich469, from the Biotechnology Program (contract ERBBIO4-CT960464) of the European Union, and from the Fonds der Chemischen Industrie (W.B.) and the SFBs 223 and 549 (H.T.) is greatly acknowledged.

1 Woessner J. F. Jr. (1991) Matrix metalloproteinases and their inhibitors in connective tissue remodeling. FASEB J. **5:** 2145–2155

2 Nagase, H., Das, S. K., Dey, S. K., Fowlkes, J. L., Huang, W. and Brew, K. (1997) In: Inhibitors of Metalloproteinases in Development and Disease, Hawkes S. P., Edwards D. R. and Khokha R. (eds), Harwood, Lausanne
3 Johnson L. L., Dyer R. and Hupe D. J. (1998) Matrix metalloproteinases. Curr. Opin. Chem. Biol. **2:** 466–471
4 Yong V. W., Krekoski C. A., Forsyth P. A., Bell R. and Edwards D. R. (1998) Matrix metalloproteinases and diseases of the CNS. Trends Neurosci. **21:** 75–80
5 Coussens L. M. and Werb Z. (1996) Matrix metalloproteinases and the development of cancer. Chem. Biol. **3:** 895–904
6 Chambers A. F. and Matrisian L. M. (1997) Changing views of the role of matrix metalloproteinases in metastasis. J. Natl. Cancer Inst. **89:** 1260–1270
7 Beckett R. and Whittaker M. (1998) Matrix metalloproteinase inhibitors 1998. Exp. Opin. Ther. Patents **8:** 259–282
8 Bottomley K. M., Johnson W. H. and Walter D. S. (1998) Matrix metalloproteinase inhibitors in arthritis. J. Enz. Inhib. **13:** 79–101
9 Massova I., Kotra L. P., Fridman R. and Mobashery S. (1998) Matrix metalloproteinases: structures, evolution and diversification. FASEB J. **12:** 1075–1095
10 Rawlings N. D. and Barrett A. J. (1995) Evolutionary families of metallopeptidases. Methods Enzymol. **248:** 183–229
11 Sang Q. A. and Douglas D. A. (1996) Computational sequence analysis of matrix metalloproteinases. J. Prot. Chem. **15:** 137–160
12 Murphy G. J., Murphy G. and Reynolds J. J. (1991) The origin of matrix metalloproteinases and their familial relationships. FEBS Lett. **289:** 4–7
13 Sato H., Takino T., Okada Y., Cao J., Shinagawa A., Yamamoto E. et al. (1994) A matrix metalloproteinase expressed on the surface of invasive tumour cells. Nature **370:** 61–65
14 Sato H., Kinoshita T., Takino T., Nakayama K. and Seiki M. (1996) Activation of a recombinant membrane type 1-matrix metalloproteinase (MT1-MMP) by furin and its interaction with tissue inhibitor of metalloproteinases (TIMP)-2. FEBS Lett. **393:** 101–104
15 Pei D. and Weiss S. J. (1996) Transmembrane-deletion mutants of the membrane-type matrix metalloproteinase-1 process progelatinase A and express intrinsic matrix-degrading activity. J. Biol. Chem. **271:** 9135–9140
16 Murphy G. and Knäuper V. (1997) Relating matrix metalloproteinase structure to function: why the 'hemopexin' domain? Matrix Biol. **15:** 511–518
17 Goldberg G. I., Wilhelm S. M., Kronberger A., Bauer E. A., Grant G. A. and Eisen A. Z. (1986) Human fibroblast collagenase. Complete primary structure and homology to an oncogene transformation-induced rat protein. J. Biol. Chem. **261:** 6600–6605
18 Wilhelm S. M., Collier I. E., Kronberger A., Eisen A. Z., Marmer B. L., Grant G. A. et al. (1987) Human skin fibroblast stromelysin: structure, glycosylation, substrate specificity and differential expression in normal and tumorigenic cells. Proc. Natl. Acad. Sci. USA **84:** 6725–6729
19 Muller D., Quantin B., Gesnel M.-C., Millon-Collard R., Abecassis J. and Breathnach R. (1988) The collagenase gene family in humans consists of at least four members. Biochem. J. **253:** 187–192
20 Hasty K. A., Pourmotabbed T. F., Goldberg G. I., Thompson J. P., Spinella D. G., Stevens R. M. et al. (1990) Human neutrophil collagenase. A distinct gene product with homology to other metalloproteinases. J. Biol. Chem. **265:** 11421–11424
21 Okada A., Bellocq J.-P., Royer N., Chenard M.-P., Rio M.-C., Chambon P. et al. (1995) Membrane-type matrix metalloproteinase (MT-MMP) gene is expressed in stromal cells of human colon, breast and head and neck carcinomas. Proc. Natl. Acad. Sci. USA **92:** 2730–2734
22 Fernandez-Catalan C., Bode W., Huber R., Turk D., Calvete J. J., Lichte A. et al. (1998) Crystal structure of the complex formed by the membrane type 1-matrix metalloproteinase with the tissue inhibitor of metalloproteinases-2, the soluble progelatinase A receptor. EMBO J. **17:** 5238–5248
23 Douglas D. A., Shi Y. E. and Sang Q. A. (1997) Computational sequence analysis of the tissue inhibitor of metalloproteinase family. J. Prot. Chem. **16:** 237–255
24 Gomez D. E., Alonso D. F., Yoshiji H. and Thorgeirsson U. P. (1997) Tissue inhibitors of metalloproteinases: structure, regulation and biological functions. Eur. J. Cell Biol. **74:** 111–122
25 Cawston T. (1998) Matrix metalloproteinases and TIMPs: properties and implications for the rheumatic diseases. Mol. Med. Today **4:** 130–137
26 Butler G. S., Will H., Atkinson S. J. and Murphy G. (1997) Membrane-type-2 matrix metalloproteinase can initiate the processing of progelatinase A and is regulated by the tissue inhibitors of metalloproeinases. Eur. J. Biochem. **244:** 653–657
27 Will H., Atkinson S. J., Butler G. S., Smyth B. and Murphy G. (1996) The soluble catalytic domain of membrane type 1 matrix metalloproteinase cleaves the propeptide of progelatinase A and initiates autocatalytic activation. J. Biol. Chem. **271:** 17119–17123
28 Zucker S., Drews M., Conner C., Foda H. D., DeClerck Y. A., Langley K. E. et al. (1998) Tissue inhibitor of metalloproteinase-2 (TIMP-2) binds to the catalytic domain of the cell surface receptor, membrane type 1-matrix metalloproteinase 1 (MT1-MMP). J. Biol. Chem. **273:** 1216–1222
29 Murphy G. and Willenbrock F. (1995) Tissue inhibitors of matrix metalloendopeptidases. Methods Enzymol. **248:** 496–510
30 Strongin A. Y., Collier I. E., Bannikov U., Marmer B. L., Grant G. A. and Goldberg G. I. (1995) Mechanism of cell surface activation of 72-kDa type IV collagenase. J. Biol. Chem. **270:** 5331–5338
31 Strongin A. Y., Marmer B. L., Grant G. A. and Goldberg G. I. (1993) Plasma membrane-dependent activation of the 72-kDa type IV collagenase is prevented by complex formation with TIMP-2. J. Biol. Chem. **268:** 14033–14039
32 Kinoshita T., Sato H., Takino T., Itoh M., Akizawa T. and Seiki M. (1996) Processing of a precursor of 72-kilodalton type IV collagenase/gelatinase A by a recombinant membrane-type 1 matrix metalloproteinase. Cancer Res. **56:** 2535–2538
33 Huang W., Meng Q., Suzuki K., Nagase H. and Brew K. (1997) Mutational study of the amino-terminal domain of human tissue inhibitor of metalloproteinases 1 (TIMP-1) locates an inhibitory region for matrix metalloproteinases. J. Biol. Chem. **272:** 22086–22091
34 Murphy G., Houbrechts A., Cockett M. I., Williamson R. A., O'Shea M. and Docherty A. J. P. (1991) The N-terminal domain of human tissue inhibitor of metalloproteinases retains metalloproteinase inhibitory activity. Biochemistry **30:** 8097–8102
35 Lovejoy B., Cleasby A., Hassell A. M., Longley K., Luther M. A., Weigl D. et al. (1994) Structure of the catalytic domain of fibroblast collagenase complexed with an inhibitor. Science **263:** 375–377
36 Borkakoti N., Winkler F. K., Williams D. H., D'Arcy A., Broadhurst M. J., Brown P. A. et al. (1994) Structure of the catalytic domain of human fibroblast collagenase complexed with an inhibitor. Nature Struct. Biol. **1:** 106–110
37 Stams T., Spurlino J. C., Smith D. L., Wahl R. C., Ho T. F., Qoronfleh M. W. et al. (1994) Structure of human neutrophil collagenase reveals large S1′ specificity pocket. Nature Struct. Biol. **1:** 119–123
38 Bode W., Reinemer P., Huber R., Kleine T., Schnierer S. and Tschesche H. (1994) The X-ray crystal structure of the catalytic domain of human neutrophil collagenase inhibited by a substrate analogue reveals the essentials for catalysis and specificity. EMBO J. **13:** 1263–1269
39 Reinemer P., Grams F., Huber R., Kleine T., Schnierer S., Pieper M. et al. (1994) Structural implications for the role of the N-terminus in the 'superactivation' of collagenases—a crystallographic study. FEBS Lett. **338:** 227–233

40 Gooley P. R., O'Connell J. F., Marcy A. I., Cuca G. C., Salowe S. P., Bush B. L. et al. (1994) NMR structure of inhibited catalytic domain of human stromelysin-1. Nature Struct. Biol. **1:** 111–118

41 Lovejoy B., Hassell A. M., Luther M. A., Weigl D. and Jordan S. R. (1994) Crystal structures of recombinant 19-kDa human fibroblast collagenase complexed to itself. Biochemistry **33:** 8207–8217

42 Spurlino J. C., Smallwood A. M., Carlton D. D., Banks T. M., Vavra K. J., Johnson J. S. et al. (1994) 1.56 Å structure of mature truncated human fibroblast collagenase. Proteins: Struct. Funct. Genet. **19:** 98–109

43 Browner M. F., Smith W. W. and Castelhano A. L. (1995) Matrilysin-inhibitor complexes: common themes among metalloproteases. Biochemistry **34:** 6602–6610

44 Becker J. W., Marcy A. I., Rokosz L. L., Axel M. G., Burbaum J. J., Fitzgerald P. M. D. et al. (1995) Stromelysin-1: three-dimensional structure of the inhibited catalytic domain and of the C-truncated proenzyme. Prot. Sci. **4:** 1966–1976

45 Dhanaraj V., Ye Q.-Z., Johnson L. L., Hupe D. J., Ortwine D. F., Dunbar J. B. et al. (1996) X-ray structure of a hydroxamate inhibitor complex of stromelysin catalytic domain and its comparison with members of the zinc metalloproteinase superfamily. Structure **4:** 375–386

46 vanDoren S. R., Kurochkin A. V., Hu W., Ye Q. Z., Johnson L. L., Hupe D. J. et al. (1995) Solution structure of the catalytic domain of human stromelysin complexed with a hydrophobic inhibitor. Protein Sci. **4:** 2487–2498

47 Wetmore D. R. and Hardman K. D. (1996) Roles of the propeptide and metal ions in the folding and stability of the catalytic domain of stromelysin (matrix metalloproteinase 3). Biochemistry **35:** 6549–6558

48 Gomis-Rüth F. X., Maskos K., Betz M., Bergner A., Huber R., Suzuki K. et al. (1997) Mechanism of inhibition of the human matrix metalloproteinase stromelysin-1 by TIMP-1. Nature **389:** 77–81

49 Grams F., Reinemer P., Powers J. C., Kleine T., Pieper M., Tschesche H. et al. (1995) X-ray structures of human neutrophil collagenase complexed with peptide hydroxamate and peptide thiol inhibitors. Implications for substrate binding and rational drug design. Eur. J. Biochem. **228:** 830–841

50 Grams F., Crimmin M., Hinnes L., Huxley P., Pieper M., Tschesche H. et al. (1995) Structure determination and analysis of human neutrophil collagenase complexed with a hydroxamate inhibitor. Biochemistry **34:** 14012–14020

51 Li J.-Y., Brick P., O'Hare M. C., Skarzynski T., Lloyd L. F., Curry V. A. et al. (1995) Structure of full-length porcine synovial collagenase reveals a C-terminal domain containing a calcium-linked, four-bladed β-propeller. Structure **3:** 541–549

52 Libson A., Gittis A., Collier I., Marmer B., Goldberg G. and Lattman E. E. (1995) Crystal structure of the hemopexin-like C-terminal domain of gelatinase A. Nature Struct. Biol. **2:** 938–942

53 Gohlke U., Gomis-Rüth F.-X., Crabbe T., Murphy G., Docherty A. J. P. and Bode W. (1996) The C-terminal (haemopexin-like) domain structure of human gelatinase A (MMP2): structural implications for its function. FEBS Lett. **378:** 126–130

54 Gomis-Rüth F. X., Gohlke U., Betz M., Knäuper V., Murphy G, Lopez-Otin C. et al. (1996) The helping hand of collagenase-3 (MMP-13): 2.7 Å crystal structure of its C-terminal haemopexin-like domain. J. Mol. Biol. **264:** 556–566

55 Bode W. (1995) A helping hand for collagenases: the haemopexin-like domain. Structure **3:** 527–530

56 Williamson R. A., Martorell G., Carr M. D., Murphy G., Docherty A. J., Freedman R. B. et al. (1994) Solution structure of the active domain of tissue inhibitor of metalloproteinases-2. A new member of the OB fold protein family. Biochemistry **33:** 11745–11759

57 Williamson R. A., Carr M. D., Frenkiel T. A., Feeney J. and Freedman R. B. (1997) Mapping the binding site for matrix metalloproteinase on the N-terminal domain of the tissue inhibitor of metalloproteinases-2 by NMR chemical shift perturbation. Biochemistry **36:** 13882–13889

58 Muskett F. W., Frenkiel T. A., Feeney J., Freedman R. B., Carr M. D. and Williamson R. (1998) High resolution structure of the N-terminal domain of tissue inhibitor of metalloproteinases-2 and characterization of its interaction site with matrix metalloproteinase-3. J. Biol. Chem. **273:** 21736–21743

59 Schechter I. and Berger A. (1967) On the size of the active site in proteases. I. Papain. Biochem. Biophys. Res. Commun. **27:** 157–162

60 Bode W., Gomis-Rüth F.-X. and Stöcker W. (1993) Astacins, serralysins, snake venom and matrix metalloproteinases exhibit identical zinc-binding environments (HEXXHXXGXXH and Met-turn) and topologies and should be grouped into a common family, the 'metzincins'. FEBS Lett. **331:** 134–140

61 Stöcker W., Grams F., Baumann U., Reinemer P., Gomis-Rüth F. X., McKay D. B. et al. (1995) The metzincins—topological and sequential relations between the astacins, adamalysins, serralysins, and matrixins (collagenases) define a superfamily of zinc-peptidases. Protein Sci. **4:** 823–840

62 Pickford A. R., Potts J. R., Bright J. R., Phan I. and Campbell I. D. (1997) Solution structure of a type 2 module from fibronectin: implications for the structure and function of the gelatin-binding domain. Structure **5:** 359–370

63 Knäuper V., Murphy G. and Tschesche H. (1996) Activation of human neutrophil procollagenase by stromelysin 2. Eur. J. Biochem. **235:** 187–191

64 Suzuki K., Enghild J. J., Morodomi T., Salvesen G. and Nagase H. (1990) Mechanisms of activation of tissue procollagenase by matrix metalloproteinase 3 (stromelysin). Biochemistry **29:** 10261–10270

65 Nagase H. (1997) Activation mechanisms of matrix metalloproteinases. Biol. Chem. **378:** 151–160

66 Pieper M., Betz M., Budisa N., Gomis-Rüth F.-X., Bode W. and Tschesche H. (1997) Expression, purification, characterization and X-ray analysis of selenomethionine 215 variant of leukocyte collagenase. J. Protein Chem. **16:** 637–650

67 Netzel-Arnett S., Fields G. B., Birkedal-Hansen H. and van Wart H. E. (1991) Sequence specificities of human fibroblast and neutrophil collagenase. J. Biol. Chem. **266:** 6747–6755

68 Netzel-Arnett S., Sang Q. X., Moore W. G. I., Navre M., Birkedal-Hansen H. and van Wart H. E. (1993) Comparative sequence specificities of human 72- and 92-kDa gelatinases (type IV collagenases) and PUMP (matrilysin). Biochemistry **32:** 6427–6432

69 Niedzwiecki L., Teahan J., Harrison R. K. and Stein R. L. (1992) Substrate specificity of the human matrix metalloproteinase stromelysin and the development of continuous fluoremetric assays. Biochemistry **31:** 12618–12623

70 Birkedal-Hansen H., Moore W. G. I., Bodden M. K., Windsor L. J., Birkedal-Hansen B., DeCarlo A. et al. (1993) Matrix metalloproteinases: a review. Crit. Rev. Oral Biol. Med. **4:** 197–250

71 Matthews B. W. (1988) Structural basis of the action of thermolysin and related zinc peptidases. Acc. Chem. Res. **21:** 333–340

72 Crabbe T., Zucker S., Cockett M. I., Willenbrock F., Tickle S., O'Connell J. P. et al. (1994) Mutation of the active site glutamic acid of human gelatinase A: effects on latency, catalysis and the binding of tissue inhibitor of metalloproteinases-1. Biochemistry **33:** 6684–6690

73 Windsor L. J., Bodden M. K., Birkedal-Hansen B., Engler J. A. and Birkedal-Hansen H. (1994) Mutational analysis of residues in and around the active site of human fibroblast-type collagenase. J. Biol. Chem. **269:** 26201–26207

74 Bode W., Gomis-Rüth F. X., Huber R., Zwilling R. and Stöcker W. (1992) Structure of astacin and implications for activation of astacins and zinc ligation of collagenases. Nature **358:** 164–166

75 Grams F., Dive V., Yiotakis A., Yiallouros I., Vassiliou S., Zwilling R. et al. (1996) Structure of astacin with a transition-state analogue inhibitor. Nature Struct. Biol. **3:** 671–675

76 Noel A., Santavicca M., Stoll I., L'Hoir C., Staub A., Murphy G. et al. (1995) Identification of structural determinants controlling human and mouse stromelysin-3 proteolytic activities. J. Biol. Chem. **270:** 22866–22872
77 Nicholls A., Bharadwaj R. and Honig B. (1993) Grasp—graphical representation and analysis of surface properties. Biophys. J. **64:** A166
78 van Wart H. E. and Birkedal-Hansen H. (1990) The cysteine switch: a principle of regulation of metalloproteinase activity with potential applicability to the entire matrix metalloproteinase gene family. Proc. Natl. Acad. Sci. USA **87:** 5578–5582
79 Faber H. R., Groom C. R., Baker H. M., Morgan W. T., Smith A. and Baker E. N. (1995) 1.8 Å crystal structure of the C-terminal domain of rabbit serum haemopexin. Structure **3:** 551–559
80 Murphy G., Allan J. A., Willenbrock F., Cockett M. I., O'Connell J. P. and Docherty A. J. P. (1992) The role of the C-terminal domain in collagenase and stromelysin specificity. J. Biol. Chem. **267:** 9612–9618
81 Sanchez-Lopez R., Alexander C. M., Behrendtsen O., Breathnach R. and Werb Z. (1993) Role of zinc-binding- and hemopexin domain-encoded sequences in the substrate specificity of collagenase and stromelysin-2 as revealed by chimeric proteins. J. Biol. Chem. **268:** 7238–7247
82 Hirose T., Patterson C., Pourmotabbed T., Mainardi C. L. and Hasty K. A. (1993) Structure-function relationship of human neutrophil collagenase: identification of regions responsible for substrate specificity and general proteinase activity. Proc. Natl. Acad. Sci. USA **90:** 2569–2573
83 Ohuchi E., Imai K., Fujii Y., Sato H., Seiki M. and Okada Y. (1997) Membrane type 1 matrix metalloproteinase digests interstitial collagens and other extracellular matrix macromolecules. J. Biol. Chem. **272:** 2446–2451
84 Knäuper V., Docherty A. J. P., Smith B., Tschesche H. and Murphy G. (1997) Analysis of the contribution of the hinge region of human neutrophil collagenase (HNC, MMP-8) to stability and collagenolytic activity by alanine scanning mutagenesis. FEBS Lett. **405:** 60–64
85 Ottl J., Battistuta R., Pieper M., Tschesche H., Bode W., Kühn K. et al. (1996) Design and synthesis of heterotrimeric collagen peptides with a built-in cystine knot. FEBS Lett. **398:** 31–36
86 Cao J., Sato H., Takino T. and Seiki M. (1995) The C-terminal region of membrane type matrix metalloproteinase is a functional transmembrane domain required for progelatinase A activation. J. Biol. Chem. **270:** 801–805
87 Butler G. S., Butler M. J., Atkinson S. J., Will H., Tamura T., van Westrum S. S. et al. (1998) The TIMP2 membrane type 1 metalloproteinase 'receptor' regulates the concentration and efficient activation of progelatinase A. J. Biol. Chem. **273:** 871–880
88 Evans S. V. (1993) SETOR: hardware lighted three-dimensional solid model representations of macromolecules. J. Mol. Graph. **11:** 134–138
89 Barton G. J. (1993) ALSCRIPT: a tool to format multiple sequence alignments. Protein Eng. **6:** 37–40